Enhancement in ferroelectricity in V-doped ZnO thin film grown using laser ablation

Tara Dhakal, Devajyoti Mukherjee, Robert Hyde, Hariharan Srikanth, Pritish Mukherjee and Sarath Witanachchi

Department of Physics and Center of Integrated Functional Materials, University of South Florida, Tampa, FL 33620

UNIVERSITY OF SOUTH FLORIDA

LAMSAT Laboratory for Advanced Materials Science and Technology

1. Introduction

Wide band gap semiconductor ZnO has Multifunctionality :

Piezoelectricity [1], Ferromagnetism [2], Optoelectronics [3], Gas sensor [4], Photocatalysis [5], Sensors and Actuators [6]

Our Goal : Spontaneous Polarization in ZnO

- ZnO has hexagonal structure
- ZnO is non-centrosymmetric
- Zinc has 2^+ valence state in ZnO
- Replacing Zn^{2+} by smaller cation with different valence state would create charge polarity and strain in the Zn-O bond, which in turn gives Spontaneous Polarization
- Growing ZnO films in oxygen rich ambient makes the material more insulating which enhances switching

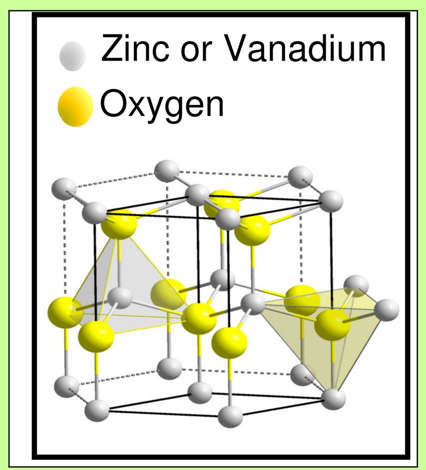

Fig.1: Wurtzite ZnO Unit Cell [7]

Recent work

- Yang et al. [8,9] has reported a switchable spontaneous polarization in 2.5 at. % V-doped ZnO
- A butterfly like displacement graph is reported as signature of spontaneous polarization as shown in Fig.2
- The effective d_{33} coefficient of V-doped ZnO is reported to be as high as 110pC/N. This value is an order higher compared to the d_{33} coefficient of bulk ZnO [10] which is 9.9 pC/N

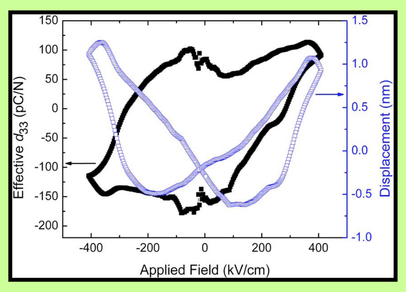

Fig.2: The d_{33} hysteresis loop of $Zn_{0.975}V_{0.025}O$ film [8]

d_{33} in the ferroelectrics can be expressed

$$d_{33} = 2Q_{eff}\varepsilon_o\varepsilon_r P$$

where Q_{eff} is effective electrostriction coefficient , ε_o and ε_r are free and relative permittivity and P is the polarization

Switchable d_{33} ⟹ Switchable P

Our Plan

- Grow 2 at. % V doped ZnO thin film at higher O_2 pressure
- Enhance O_2 Intensity for better Oxygen incorporation in the film

2. Experimental Details

Dual-Laser PLD with ICCD Imaging System

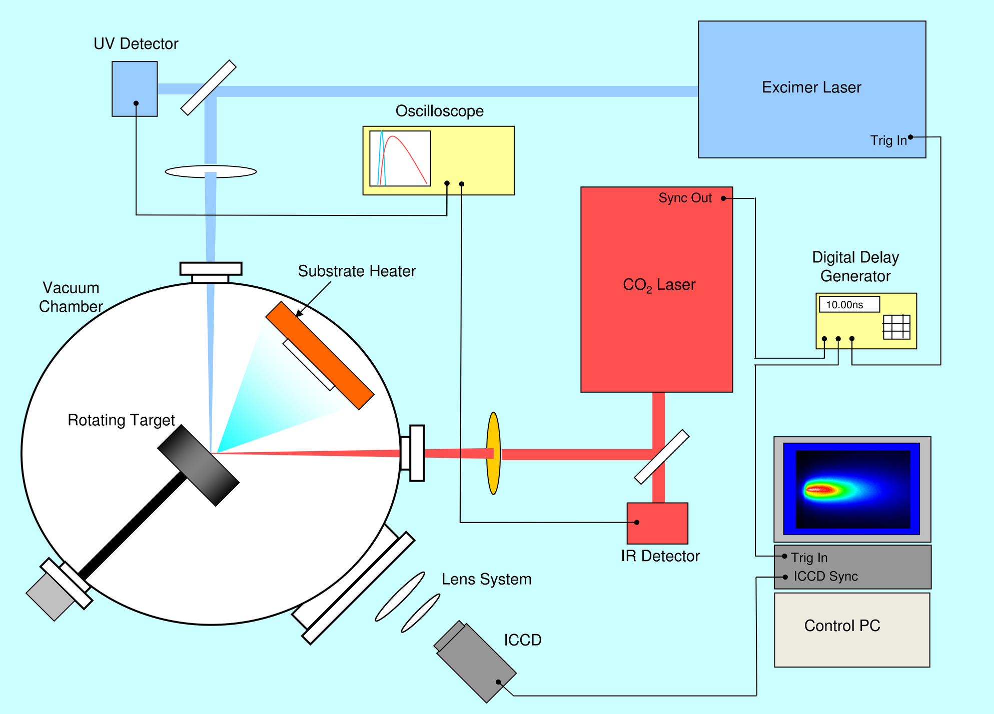

Fig.3 : The schematic diagram of the dual-laser deposition system (248 nm KrF excimer laser and 10.6 μm CO_2 laser) with the ICCD imaging system (PI-MAX:512 UNIGEN)

Laser Target Interaction

Laser pulses of varying fluences were impinged on the fresh target surfaces to study the target surface morphology by using SEM and the stoichiometry by using Energy Dispersive Spectroscopy (EDS). The melted surface due to laser ablation showed smooth surface with Hexagonal facets characteristic of ZnO. The Vanadium content in the target for all the fluences remained nearly same

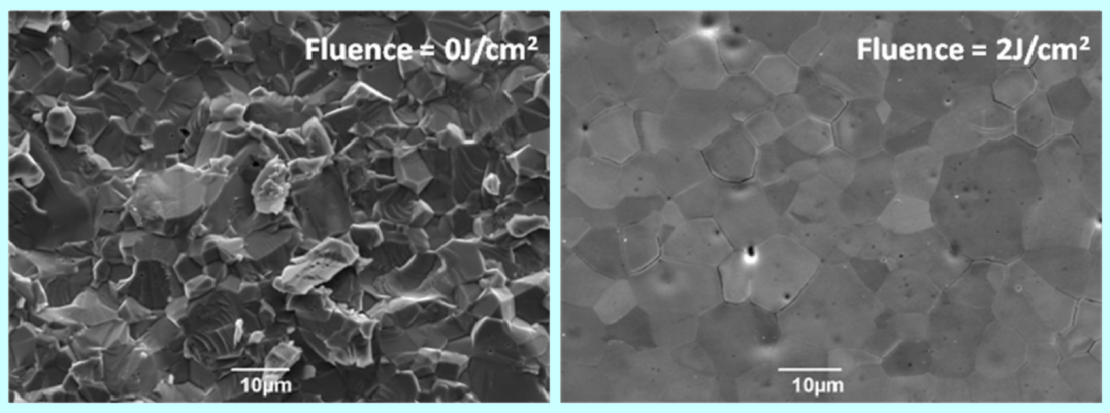

Fig.4 : SEM pictures of unablated (left) and 2J/cm² ablated (right) surface of ZnO ceramic target

3. Thin Film Growth

Plume propagation by single laser 2 J/cm² UV excimer fluence at 1200 ns step

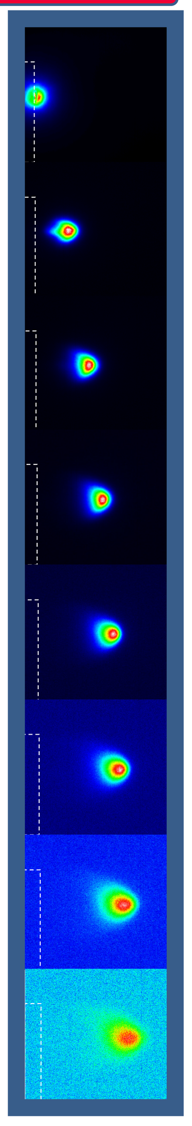

Plume profile vs. film quality

Total emission intensity for 100 mT O_2 is the highest indicating higher ionization concentration. As the O_2 pressure increased, the plume is more directed and more particles appeared on the surface as shown below [11]

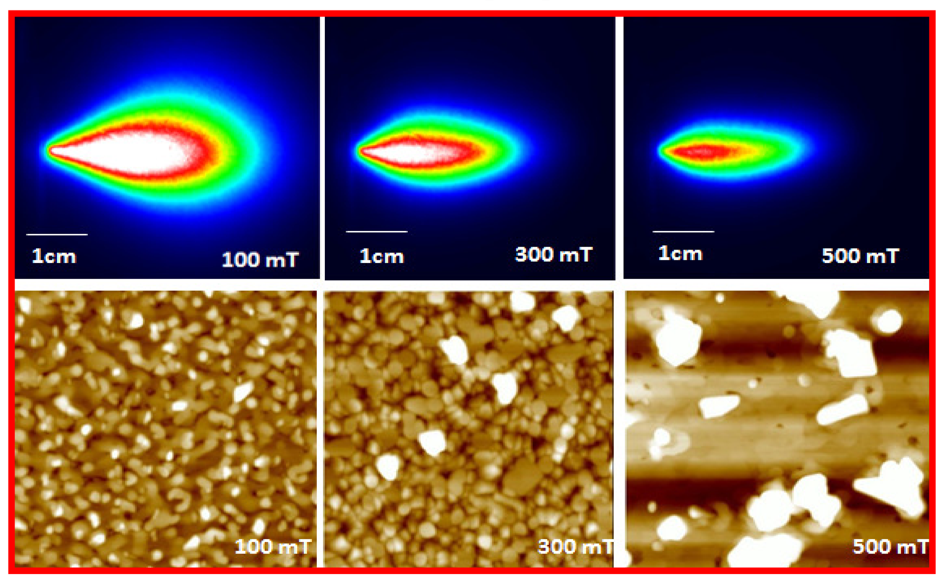

Fig. 5 : Plume images taken by ICCD for various O_2 pressures - 100mT, 300mT and 500mT. The lower panel shows the corresponding AFM images (5μm x 5μm) of the films grown on c-cut sapphire (Al_2O_3) substrates heated at 600℃

X-ray Diffraction

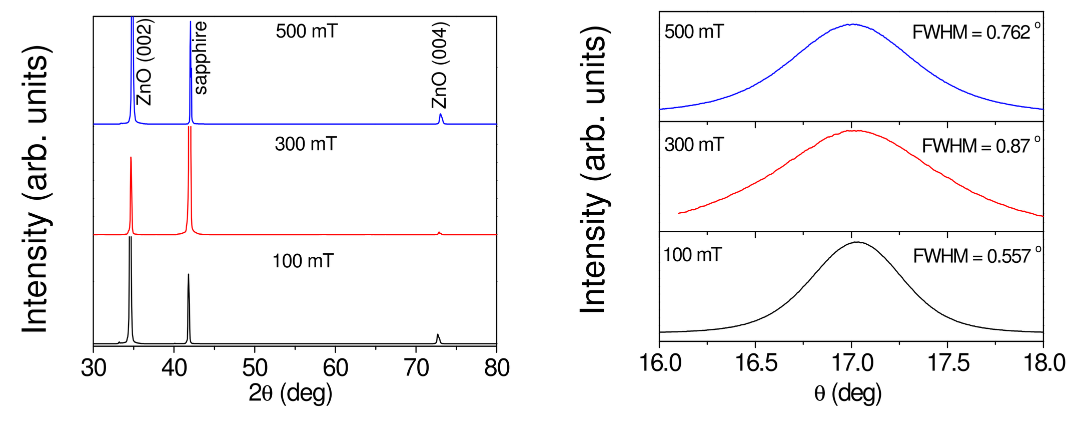

Figure 6: XRD peaks of 2 at. % V-doped ZnO grown on c-cut sapphire substrate. The right panel shows the rocking curves of (002) ZnO peak showing FWHMs.

Future film growth using Dual Laser System

- Plume profile becomes broader with dual laser
- Plasma Intensity increases which will better incorporate oxygen into the film

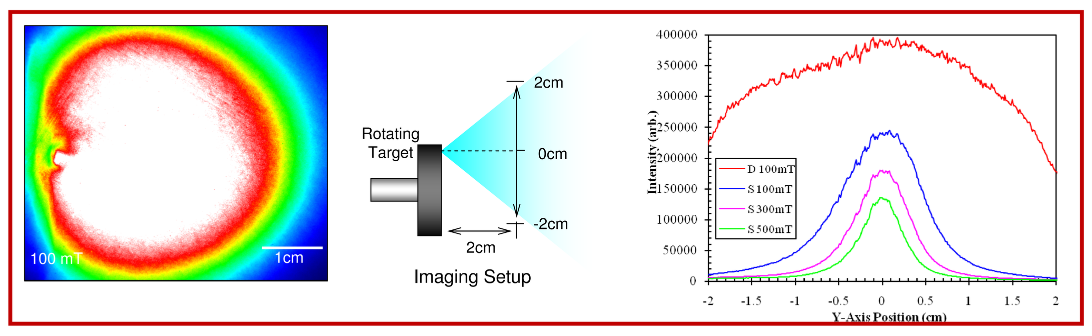

Figure 7: ICCD imaging (left) , image set up (middle) and total emission intensity plot for single-laser 2 J/cm² (100 mT O_2, 300mT O_2 and 500 mT O_2) and dual laser (2J/cm² UV and 2J CO_2) at 100 mT O_2. Intensity range is from 0 to 300000

4. Resistivity measurements

- Van der Pauw method was used
- The higher the O_2 pressure, more insulating were the films
- Hall voltage measurement showed n-type

The carrier concentration (n) was obtained from the following equation

$$n = \frac{IB}{qV_H}$$

where I is current, B is applied field , q is electronic charge and V_H is hall Voltage

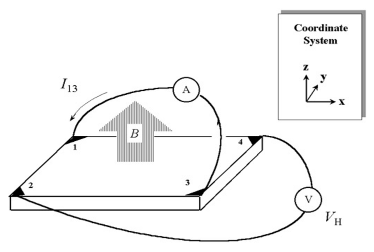

Fig.8 : Schematic of a van der Pauw configuration [12]

Table 1: Resistivity and Hall measurement using Vander Paw Technique

Background Pressure (mT)	Sheet resistance $R_S(\Omega)$	Resistivity $\rho(\Omega cm)$	Carrier Conc. n_C (cm^{-3})	Mobility μ_H (cm^2/Vs)
100	2.76×10^2	8.82×10^{-3}	2.66×10^{19}	26.51
200	2.38×10^5	7.61	3.08×10^{17}	2.67
300	1.19×10^7	4.53×10^2	3.76×10^{15}	3.65

5. Electric Polarization

- Standard Sawyer-Tower circuit is used for polarization measurement

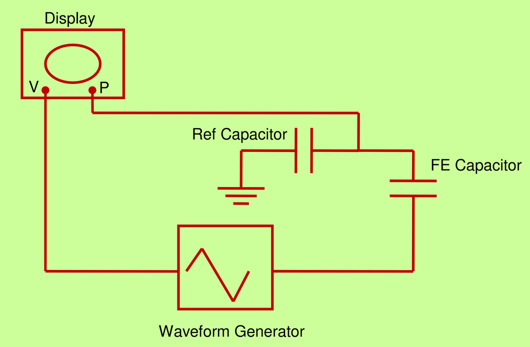

The charge on the FE capacitor

Q=CV

where C = reference capacitor and V = voltage across the reference capacitor

Thus P = Q/A

where A is the area of capacitor

- The films grown at higher Oxygen pressure exhibited Higher electric polarization as shown below

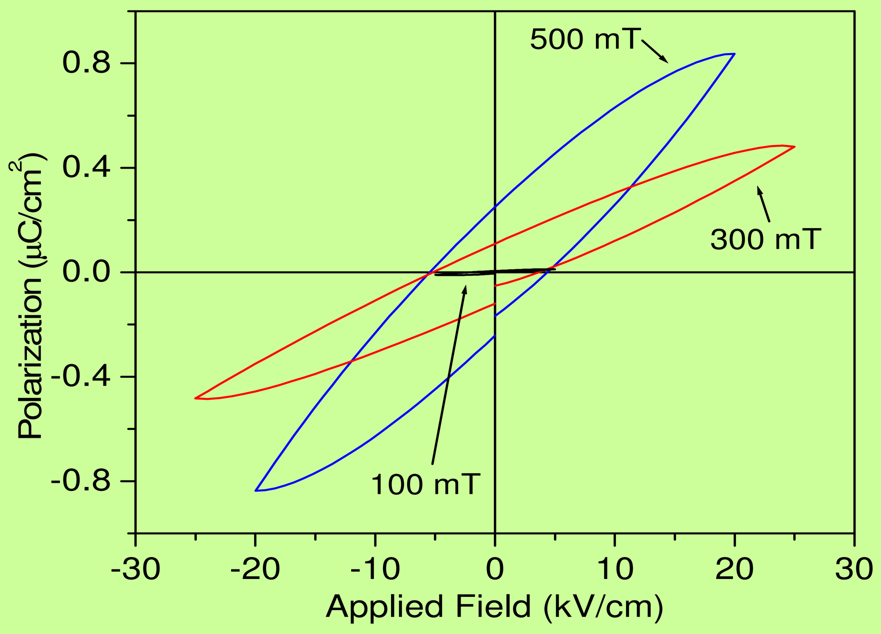

Fig. 10: Electric Polarization as a function of applied electric field for the films grown at various oxygen pressures. The polarization measurements were performed using Precision LC from Radiant Technologies

Table 2: Saturation and remanant polarization and coercivities

Background Pressure (mT)	Saturation Polarization P_S ($\mu C/cm^2$)	Remnant Polarization P_R ($\mu C/cm^2$)	Coercive Field E_C (kV/cm)
100	0.01	0.0045	2.05
300	0.48	0.1	4.4
500	0.83	0.24	4.9

6. Conclusion

- Ferroelectric switching obtained in ZnO by doping it V^{5+} ion.
- Higher saturation polarization for films grown at high O_2 pressure
- The ICCD imaging of the plume expansion
  - Broader for low O_2 pressure
  - Narrower for high O_2 pressure
- Ablated plume with broader expansion and higher intensity yielded smoother films
- Dual laser (UV+CO_2) will be used to grow films with reduced roughness

7. References

1. A. D. Corso et. al.,Physical Review B, **50**, 10175 (1994)
2. P. Sharma et. al., Nature Materials, **2**, 673 (2003)
3. R. D. Vispute et. al, Applied Physics Letter, **73**, 348 (1998)
4. Q. H. Li, T. Gao, Y. G. Wang, and T. H. Wang, Applied Physics Letter **86**, 123117 (2005)
5. Mrinal Dutta and Durga Basak, Nanotechnology **20**, 475602 (2009)
6. 7. T. Shibata et. al, Sens. Actuators, A **102**, 106 (2002)
7. http://en.wikipedia.org/w/index.php?title=Wurtzite_crystal_structure&oldid=299659846
8. Y. C. Yang et al., Appl. Phys. Lett. **92**, 012907 (2008)
9. Y. C. Yang et al., Appl. Phys. Lett. **90**, 242903, (2007)
10. M. H. Zhao et. al, Nano Lett. **4**, 587 (2004)
11. Pritish Mukherjee, John B. Cuff, and Sarath Witanachchi, Applied Surface Science, **127-129**, 620 (1998)
12. The schematic obtained from NIST

Acknowledgements ★ ★ ★ ★ ★

UNITED STATES DEPARTMENT OF DEFENSE www.defense.gov W81XWH-07-1-0708

National Science Foundation WHERE DISCOVERIES BEGIN DMI-0217939, DMI-0078917

2009 MRS fall meeting Boston, MA - November 30-December 4